Force transmissibility and vibration power flow behaviour of inerter-based vibration isolators

Jian Yang

Department of Mechanical, Materials and Manufacturing Engineering, University of Nottingham Ningbo China, 199 Taikang East Road, Ningbo 315100, China.

E-mail: jian.yang@nottingham.edu.cn

Abstract. This paper investigates the dynamics and performance of inerter-based vibration isolators. Force / displacement transmissibility and vibration power flow are obtained to evaluate the isolation performance. Both force and motion excitations are considered. It is demonstrated that the use of inerters can enhance vibration isolation performance by enlarging the frequency band of effective vibration isolation. It is found that adding inerters can introduce anti-resonances in the frequency-response curves and in the curves of the force and displacement transmissibility such that vibration transmission can be suppressed at interested excitation frequencies. It is found that the introduction of inerters enhances inertial coupling and thus have a large influence on the dynamic behaviour at high frequencies. It is shown that force and displacement transmissibility increases with the excitation frequency and tends to an asymptotic value as the excitation frequency increases. In the high-frequency range, it was shown that adding inerters can result in a lower level of input power. These findings provide a better understanding of the effects of introducing inerters to vibration isolation and demonstrate the performance benefits of inerter-based vibration isolators.

1. Introduction

There has been a growing demand for high performance vibration control devices that change the vibration transmission behaviour of dynamical systems to meet specific requirements [1, 2]. One such device is the recently proposed passive mechanical element, the inerter, which can be used to provide inertial coupling such as to modify the dynamic behaviour [3]. The forces applied on the two terminals of the device are proportional to the relative accelerations of the two ends, i.e., $F_b = b(\dot{V}_1 - \dot{V}_2)$, where F_b is the coupling inertial force, b is a parameter named inertance, $\dot{V}_1$ and $\dot{V}_2$ are the accelerations of the two ends. Since its introduction, the inerter has been employed in the design of vehicle suspension systems and building vibration control systems, etc. [4-8].

Although much work been conducted so as to improve the understanding of the effects of adding inerters to a dynamical system [9], the fundamental effects of the addition of inerters on vibration characteristics of dynamical systems still need further clarification. The performance of inerter-based vibration isolators has not been fully addressed.

It should also been pointed out that the influence of incorporating inerters on power flow behaviour of dynamical systems has been ignored in the previous investigations. Instead of individual force and displacement transmission behaviour, vibration power flows combines the effects of force and velocity in a single quantity, and can better reflect the vibration input, transmission and dissipation in a dynamical systems. The fundamental concepts of vibration power flow were proposed in [10]. Thereafter, many different approaches have been proposed to reveal power flow characteristics of

passive and active vibration control systems [11-13]. In recent years, this dynamic analysis approach has been developed to investigate vibration power flow in nonlinear dynamical systems for the application of vibration control systems and energy harvesting devices [14-18]. It is thus beneficial to examine the effects of inerters from a vibration power flow perspective for enhanced designs of inerter-based vibration isolators.

This paper aims to address the issues by investigating the influence of introducing inerters on vibration behaviour in terms of force and displacement transmissibility, as well as vibration power and energies. Both force and motion excitations will be considered. Moreover, vibration isolation performance in terms of both force and displacement transmissibility, and vibration power flow variables will be investigated and compared. Conclusions and suggestions for engineering applications are provided at the end of the paper.

2. Vibration isolation of force excitations

2.1. Force transmissibility

As shown in Fig. 1, an inerter-based vibration isolator consists of a viscous damper of damping coefficient c, a linear spring of stiffness coefficient k, and an inerter of inertance b. The mass m representing a vibrating machine is subject to a harmonic force excitation of amplitude f_0 and frequency ω. It is assumed that the inerter is ideal with negligible mass.

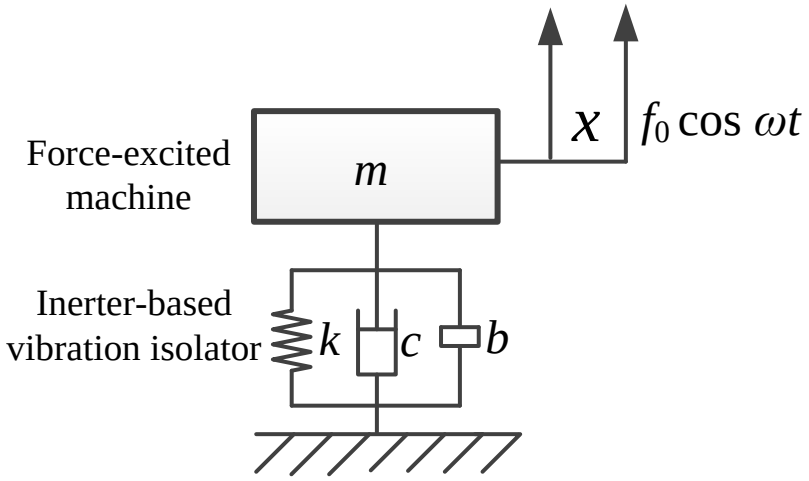

Figure 1. A schematic representation of an inerter-based vibration isolator for force excitation.

The dynamic governing equation is

$$m\ddot{x} + c\dot{x} + kx + b\ddot{x} = f_0 \cos \omega t, \tag{1}$$

By introducing non-dimensional variables

$$x_0 = \frac{mg}{k},\ \ \omega_0 = \sqrt{\frac{k}{m}},\ \tau = \omega_0 t,\ \ \xi = \frac{c}{2m\omega_0},\ \ X = \frac{x}{x_0},\ F_0 = \frac{f_0}{kx_0},\ \Omega = \frac{\omega}{\omega_0} \text{ and } \lambda = \frac{b}{m},$$

Eq. (1) can be written in a non-dimensional form:

$$(1 + \lambda)X'' + 2\xi X' + X = F_0 \cos \Omega\tau, \tag{2}$$

where the primes denote differentiation with respect to non-dimensional time τ.

The undamped natural frequency of the inerter-based isolation system is

$$\Omega_n = \sqrt{\frac{1}{1+\lambda}}. \tag{3}$$

Note that the undamped natural frequency of a conventional linear isolator (i.e., when $\lambda = 0$) is 1. Thus the addition of inerter reduces the natural frequency of the system.

Assuming that steady-state response of the mass is expressed by $X = X_0 \cos(\Omega\tau - \phi)$, the steady-state response amplitude can be obtained to be

$$r = X_0 = \frac{F_0}{\sqrt{[1-\Omega^2(1+\lambda)]^2+(2\xi\Omega)^2}}. \quad (4)$$

Fig. 2 plots the response amplitude of the isolation system against the excitation frequency. Four different values of inertance with $\lambda = 0, 1, 2$ and 5 are selected. The other parameters are set as $\xi = 0.01, F_0 = 1$. The highest resonant peak can be found when $\lambda = 5$. The figure shows that at high frequencies, the effect of inertance increases.

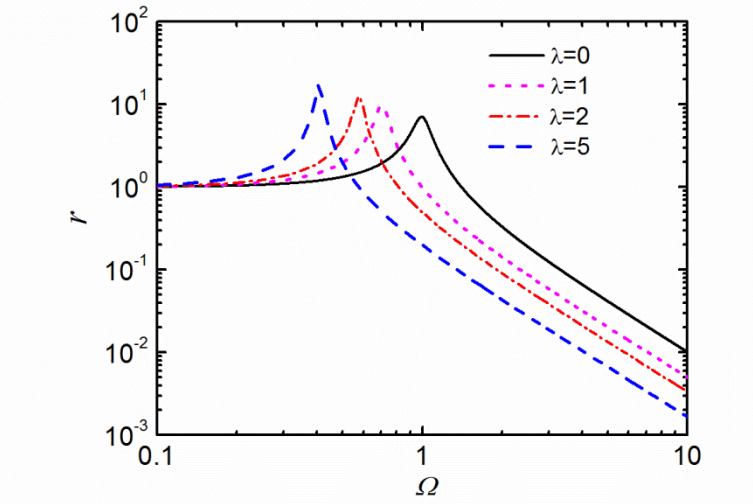

Figure 2. Response amplitude of an inerter-based isolator subject to force excitation ($\xi = 0.01, F_0 = 1$).

The non-dimensional transmitted force to the ground F_t is expressed as

$$F_t = \lambda X'' + 2\xi X' + X. \quad (5)$$

The force transmissibility TR_f is defined as the ratio of the amplitude of the transmitted force F_t to that of the excitation force:

$$TR_f = \frac{|F_t|}{F_0} = \frac{\sqrt{(2\xi\Omega)^2+(1-\lambda\Omega^2)^2}}{\sqrt{[1-\Omega^2(1+\lambda)]^2+(2\xi\Omega)^2}}. \quad (6)$$

As effective isolation of force transmission requires $TR_f < 1$, we have

$$\Omega > \sqrt{\frac{2}{1+2\lambda}}. \quad (7)$$

Thus the lower limit of the excitation frequency Ω for effective attenuation of force transmission is $\sqrt{\frac{2}{1+2\lambda}}$. It should be noted that for a conventional isolator without inerter (i.e., $\lambda = 0$), the excitation frequency Ω should be larger than $\sqrt{2}$ so as to achieve $TR_f < 1$. With use of the inerter, the lower limit of Ω is reduced, and correspondingly the frequency band for effective vibration isolation is thus enlarged. As the inertance increases, the lower limit will shift to the low frequencies.

For the undamped inerter-based vibration isolator to achieve a lower transmissibility than the case without using the inerter $\lambda = 0$, it requires

$$TR_f = \left|\frac{1-\lambda\Omega^2}{1-\Omega^2(1+\lambda)}\right| < \frac{1}{|1-\Omega^2|}, \quad (8)$$

Simplifying this expression, we have

$$\Omega_{\text{low}} = \sqrt{\frac{1+\lambda-\sqrt{1+\lambda^2}}{\lambda}} < \Omega < \sqrt{\frac{1+\lambda+\sqrt{1+\lambda^2}}{\lambda}} = \Omega_{\text{up}}. \quad (9)$$

Thus in the frequency band between Ω_{low} and Ω_{up}, the force transmissibility of the undamped inerter-based vibration isolator is lower than that of a corresponding conventional isolator. Also, the expression of TR_f for the undamped inerter-based isolator suggests that there will be a zero when $\Omega =$

$\sqrt{1/\lambda}$ and a pole at the natural frequency $\Omega = \sqrt{1/(\lambda+1)}$. The former corresponds to an anti-peak in the force transmissibility curve.

Note that in Eq. (6), the numerator and denominator are of the same order of Ω, as the non-dimensional excitation frequency Ω tends to infinity, we have

$$TR_{\text{lim}} = \lim_{\Omega\to\infty} TR = \frac{\lambda}{1+\lambda}. \tag{10}$$

Fig. 3 shows the force transmissibility characteristics of the system with $\xi = 0.01, F_0 = 1$. In the low-frequency range, the transmissibility curve of the inerter-based isolator and that of the conventional isolator merge with each other. It is also seen that the peak of the transmissibility curve shifts to the low frequencies. As suggested by expression (10), adding inerter can reduce force transmission in the frequency band between Ω_{low} and Ω_{up}. A local minimum in TR can be identified in the frequency range, suggesting an appearance of anti-resonance. For an undamped isolator, the local minimum point is located at $\Omega_{\text{anti}} = \sqrt{1/\lambda}$ and thus its value reduces as λ increases. When Ω is larger than Ω_{anti}, TR increases with the excitation frequency and tends to an asymptotic value TR_{lim}. This is in contrast to the case with $\lambda = 0$, for which the transmissibility reduces at a rate of 20dB per decade. Also, as demonstrated in Eq. (10), the asymptotic value becomes larger as λ increases but will remain smaller than 1.

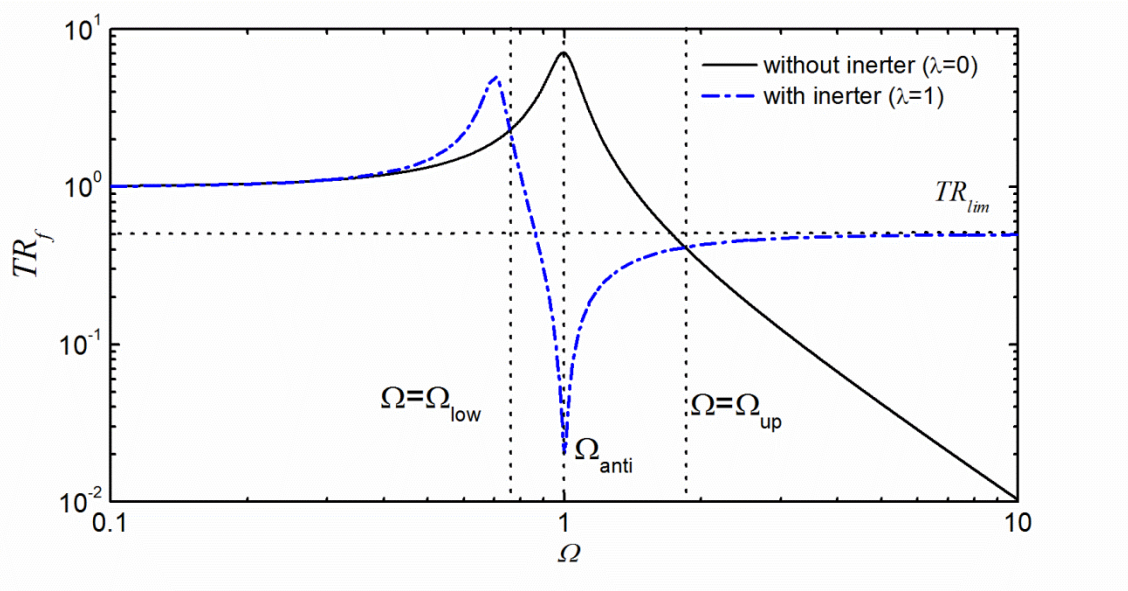

Figure 3. Force transmissibility of an inerter-based isolator subject to force excitation ($\xi = 0.01, F_0 = 1$).

2.2. Vibration power and energy

It is of interest to examine vibrational power flow behaviour of the inerter-based vibration isolator. Note that over a cycle of oscillation, the changes in the potential energy stored in the spring and the kinetic energy of the system vanish. Therefore, the non-dimensional time-averaged input power equals the non-dimensional time-averaged dissipated power:

$$\bar{p}_{in} = \bar{p}_d = \frac{1}{T}\int_0^T 2\xi X'^2 \,\mathrm{d}\tau = \xi r^2\Omega^2 = \frac{\xi F_0^2\Omega^2}{[1-\Omega^2(1+\lambda)]^2+(2\xi\Omega)^2}. \tag{11}$$

where $\bar{p}_{in}$ and $\bar{p}_d$ are time-averaged input and dissipated powers, respectively. The averaging time T is taken as $2\pi/\Omega$. In vibration isolation, the kinetic energy of the excited machine is of interest. As the velocity amplitude of the mass in the steady-state motion is $r\Omega$, the non-dimensional maximum kinetic energy of the mass in the steady-state motion is

$$K_{max} = \frac{1}{2}r^2\Omega^2 = \frac{F_0^2\Omega^2}{2\{[1-\Omega^2(1+\lambda)]^2+(2\xi\Omega)^2\}}. \tag{12}$$

After some mathematical simplification, we can find that

$$\bar{p}_{in} = \frac{\xi F_0^2}{[1-\Omega^2(1+\lambda)]^2/\Omega^2+(2\xi)^2} \leq \frac{F_0^2}{4\xi} \text{ and } K_{max} = \frac{F_0^2\Omega^2}{2\{[1-\Omega^2(1+\lambda)]^2+(2\xi\Omega)^2\}} \leq \frac{F_0^2}{8\xi^2}. \quad (13a, b)$$

The peak value of $\bar{p}_{in}$ and K_{max} is obtained when the system is excited at the undamped natural frequency $\Omega_n = \sqrt{1/(1+\lambda)}$. Also, the addition of inerter does not alter the peak value of time-averaged input power and the maximum kinetic energy. Fig. 4 shows the influence of adding inerter on the power flow behaviour of the system. Note that in the current paper, the power and energy variables are shown in a decibel scale with a reference of 10^{-12}. The parameters are set as $\xi = 0.01, F_0 = 1$ with λ varying from 0, 1, 2 and to 5. It shows that with increasing λ, the peak in each $\bar{p}_{in}$ and K_{max} curve moves to the low frequencies. As suggested by Eq. (13a, b), the peak value of power flows remains unchanged. At low excitation frequencies, $\bar{p}_{\text{in}}$ and K_{max} increase with λ. In contrast, a larger inertance λ leads to lower input power and kinetic energy at high frequencies. It suggests that in terms of power flow, adding inerter benefits vibration isolation of high-frequency excitations.

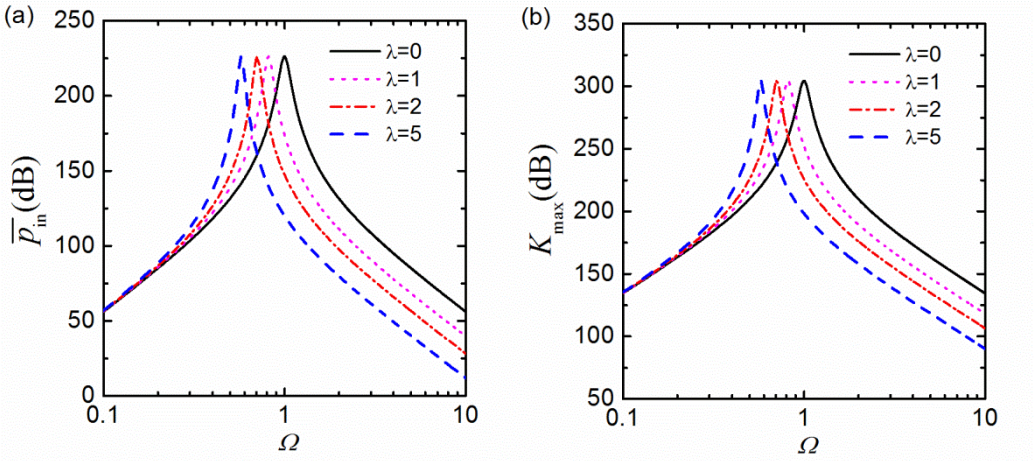

Figure 4. (a) Time-averaged input power and (b) maximum kinetic energy of the excited mass when subject to force excitations ($\xi = 0.01, F_0 = 1$).

3. Vibration isolation of base excitations

3.1. Displacement transmissibility

In some applications such as vehicles driven over uneven ground, the system is subject to base excitations and the role of isolators is to reduce the vibration transmission to the vehicle body. As shown in Fig. 5, an inerter-based vibration isolator a viscous damper of damping coefficient c, a linear spring of stiffness coefficient k, and an inerter of inertance b. Mass m represents a machine, the response of which is expected to be suppressed by adding the isolator. There is a harmonic base excitation of amplitude y_0 and frequency ω.

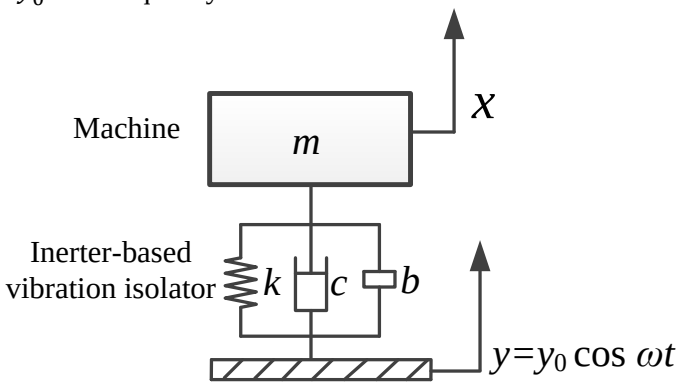

Figure 5. A schematic representation of an inerter-based vibration isolator for base excitation.

The dynamic governing equation is

$$m\ddot{x} = -c(\dot{x} - \dot{y}) - k(x - y) - b(\ddot{x} - \ddot{y}), \quad (14)$$

where x denotes the response of the machine, $y = y_0 \cos \omega t$. Introducing non-dimensional parameters: $x_0 = \frac{mg}{k}$, $\omega_0 = \sqrt{\frac{k}{m}}$, $\tau = \omega_0 t$, $\xi = \frac{c}{2m\omega_0}$, $X = \frac{x}{x_0}, Y = \frac{y}{x_0}$, $Y_0 = \frac{y_0}{x_0}$, $\Omega = \frac{\omega}{\omega_0}$ and $\lambda = \frac{b}{m}$,

Eq. (14) is transformed into a non-dimensional form

$$(1 + \lambda)X'' + 2\xi X' + X = \lambda Y'' + 2\xi Y' + Y = (1 - \lambda\Omega^2)\, Y_0 \cos \Omega\tau - 2\xi\Omega\, Y_0 \sin \Omega\tau. \quad (15)$$

where the primes denote differentiation with respect to non-dimensional time τ. It may be assumed that the response of the mass is $X = X_0 \cos(\Omega\tau - \phi)$. Inserting this expression back Eq. (15) and further simplifying, it can be found that

$$r = X_0 = \frac{Y_0\sqrt{(1-\lambda\Omega^2)^2+(2\xi\Omega)^2}}{\sqrt{[1-\Omega^2(1+\lambda)]^2+(2\xi\Omega)^2}}, \quad (16a, b)$$

Note that the numerator and denominator are of the same order of excitation frequency Ω so that we have

$$\lim_{\Omega\to\infty} r = \frac{\lambda\, Y_0}{1+\lambda}. \quad (17)$$

which shows that the response amplitude of the mass tends to a finite non-zero value as the excitation frequency tends to infinity. This behaviour is of contrast to that of a conventional isolation system. Also, for the undamped system (i.e., $\xi = 0$), r is zero when $\Omega = \sqrt{1/\lambda}$. It suggests the existence of anti-resonance in the frequency-response curve. Note that for the undamped system without inerter, the natural frequency is $\Omega_n = 1$. Thus, anti-resonance may be introduced at $\Omega_n = 1$ by adding an inerter to greatly reduce the original peak value in the frequency-response curve.

The displacement transmissibility TR_d is defined as the ratio of the response displacement amplitude of the base and that of the mass:

$$TR_d = \frac{X_0}{Y_0} = \frac{\sqrt{(1-\lambda\Omega^2)^2+(2\xi\Omega)^2}}{\sqrt{[1-\Omega^2(1+\lambda)]^2+(2\xi\Omega)^2}}, \quad (18)$$

the right-hand side of which is identical to Eq. (6) for the force excitation system. Therefore, the characteristics of TR_d with variations of λ and Ω will be the same to those of force transmissibility shown in the previous section.

3.2. Vibration power and energy

As for the power flow behaviour of the system subject to base excitation, the mechanical energy of the system remains unchanged over a cycle of oscillation, so that the non-dimensional time-averaged input power $\bar{p}_{in}$ into the system equals the time-averaged dissipated power $\bar{p}_d$ by damping, i.e.,

$$\bar{p}_{in} = \bar{p}_d. \quad (19)$$

As the non-dimensional damping force $F_d = 2\xi(X' - Y')$ and the corresponding non-dimensional velocity $V_d = (X' - Y')$, the non-dimensional time-averaged dissipated power:

$$\bar{p}_d = \frac{1}{T}\int_0^T 2\xi(X' - Y')^2\, \mathrm{d}\tau = \frac{\xi\, Y_0^2\Omega^6}{[1-\Omega^2(1+\lambda)]^2+(2\xi\Omega)^2}, \quad (20)$$

The maximum kinetic of the mass in the steady-state motion corresponds to the maximum velocity:

$$K_{max} = \frac{1}{2}X_0^2\Omega^2 = \frac{Y_0^2\Omega^2\left[\left(1-\lambda\Omega^2\right)^2+(2\xi\Omega)^2\right]}{2[1-\Omega^2(1+\lambda)]^2+2(2\xi\Omega)^2}. \quad (21)$$

Based on these Eqs. (19-21), the influence of adding an inerter on power flows of the system is examined and the results are shown in Fig. 6. The system parameters are set as $\xi = 0.01$, $Y_0 = 1$, while parameter λ varies from 0, to 1, 2 and then 5. Fig. 6(a) shows at low excitation frequencies, adding inerter has only a small influence on $\bar{p}_{in}$. A local peak can be found on each curve due to the anti-resonance introduced by the inerter. With the increase of λ, the local peak shifts to the low-frequencies. Fig. 6(b) shows the effects of adding inerter on displacement transmissibility are similar

to those on force transmissibility. There is an asymptotic value of TR_d as Ω tends to the infinity. Fig. 6(c) shows that at high frequencies, the time-averaged input power reduces as λ increases. This figure also shows that the inerter has a larger influence on time-averaged input power at high excitation frequencies. Fig. 6(d) plots the variations of the maximum kinetic energy of the machine mass m. It shows that for the isolator with inerter, there is a local minimum point of K_{max} created by anti-resonance in the frequency-response. With an increasing λ, the local minimum point moves to the low-frequencies. At high excitation frequencies, the maximum kinetic energy increases with λ.

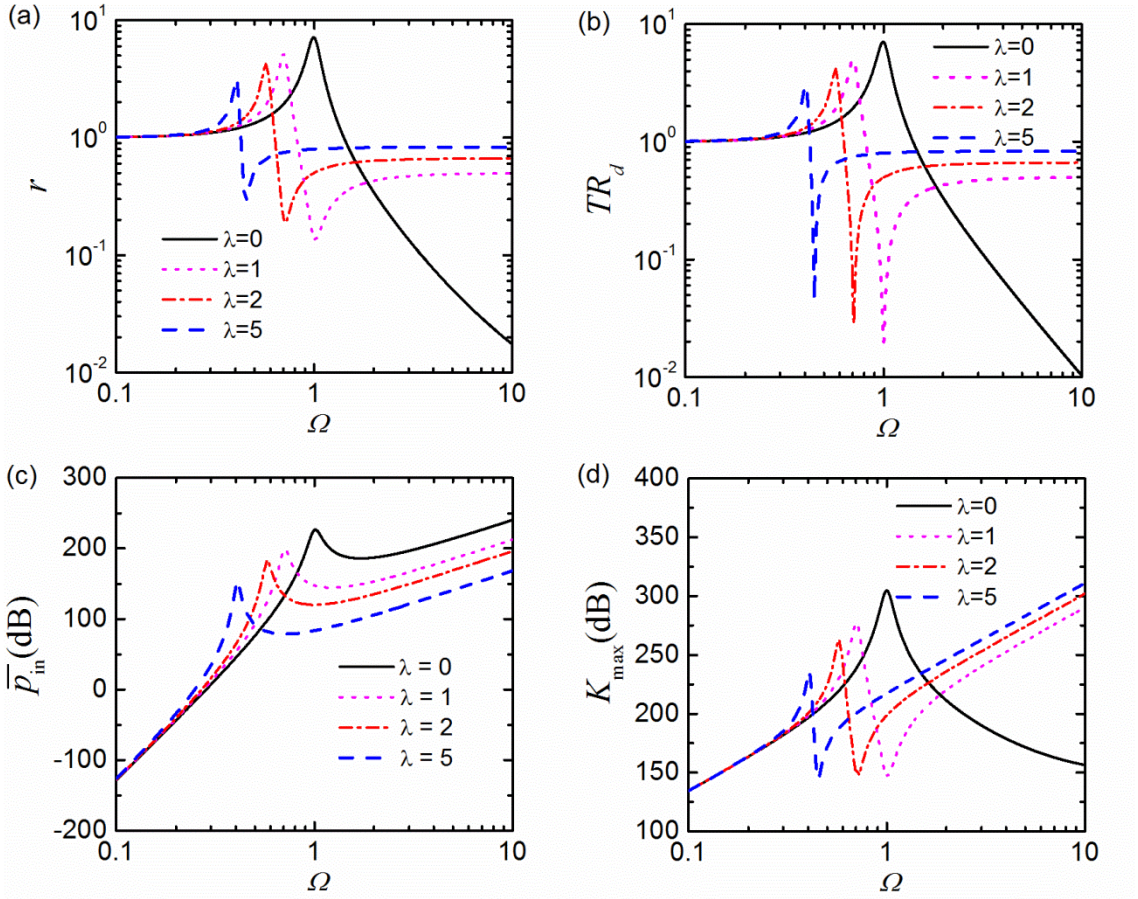

Figure 6. (a) Time-averaged input power and (b) maximum kinetic energy of an inerter-based vibration isolator subject to base excitations ($\xi = 0.01$, $Y_0 = 1$).

4. Conclusions

This paper investigated the performance of inerter-based vibration isolators. Both force / displacement transmissibility as well as vibration power flow characteristics were studied. Vibration control of systems subject to both force excitation and motion excitation is examined. It was found that adding inerters can increase inertial coupling and thus have a large influence on performance of the inerter-based isolators at high frequencies. It was also demonstrated that the addition of inerters can assist in enlarging the frequency band of effective vibration isolation. It is found that adding inerters provides anti-peaks in the frequency-response, the force and displacement transmissibility curves. This behaviour can be used to suppress peak vibration transmission at resonance by placing zeros. It was found that the introduction of inerters can results in asymptotic behaviour of force / displacement transmissibility with transmissibility tends to a fixed value when the excitation frequency tends to infinity. In the high-frequency range, it was shown that adding inerters can result in a lower time-averaged input power. These findings provide a better understanding of the functionality of inerters and can assist in vibration isolation with use of such elements.

Acknowledgments
The financial support from Ningbo Natural Science Foundation (Grant No.2015A610094) and University of Nottingham Ningbo China is greatly acknowledged.

References
[1] Ibrahim R A Recent advances in nonlinear passive vibration isolators *J. Sound Vib.* 314 (2008) 371-452
[2] Yang J, Xiong Y P and Xing J T 2013 Dynamics and power flow behaviour of a nonlinear vibration isolation system with a negative stiffness mechanism *J. Sound Vib* **332(1**) 167-183
[3] Smith M C 2002 Synthesis of mechanical networks: The inerter *IEEE T. Automat. Contr.* **47(10)** 1648-1662
[4] Smith M C and Wang F C 2004 Performance benefits in passive vehicle suspensions employing inerters *Vehicle Syst. Dyn.* **42(4)** 235–257
[5] Scheibe F and Smith M C 2009 Analytical solutions for optimal ride comfort and tyre grip for passive vehicle suspensions *Vehicle Syst. Dyn.* **47 (10)** 1229–1252
[6] Wang F C, Liao M K, Liao B H, Sue H J and Chan H A 2009 The performance improvements of train suspension systems with mechanical networks employing inerters *Vehicle Syst. Dyn.* **47(7)** 805–830
[7] Jiang J Z, Matamoros-Sanchez A Z, Goodall R N and Smith M C 2012 Passive suspensions incorporating inerters for railway vehicles *Vehicle Syst. Dyn.* **50** (Suppl. 1) 263–276
[8] Wang F C, Hong M F and Chen C W 2010 Building suspensions with inerters *P. I. Mech. Eng. C.-J. Mech.* **224 (8)** 1605–1616
[9] Chen M Z Q, Hu Y, Huang L and Chen G 2014 Influence of inerter on natural frequencies of vibration systems *J. Sound Vib.* **333** 1874-1887
[10] Goyder H G D and White R G 1980 Vibration power flow from machines into built-up structures *J. Sound Vib.* **68** 59-117
[11] Xing J T and Price W G 1999 A power-flow analysis based on continuum dynamics *Proc. R. Soc. A* **455** 401-436
[12] Xiong Y P, Xing J T and Price W G 2005 A power flow mode theory based on a system's damping distribution and power flow design approaches *Proc. R. Soc. A* **461** 3381-3411.
[13] Gardonio P, Elliott S J and Pinnington R J 1997 Active isolation of structural vibration on a multiple-degree-of-freedom system, part II: effectiveness of active control strategies *J. Sound Vib.* **16** 95-212
[14] Yang J, Xiong Y P and Xing J T 2011 Investigations on a nonlinear energy harvesting system consisting of a flapping foil and an electro-magnetic generator using power flow analysis, *Proceedings of the ASME Design Engineering Technical Conference,* Washington DC, USA,Volumn 1(Parts A and B) 317-324
[15] Yang J, Xiong Y P and Xing J T 2012 Power flow behaviour of the Duffing oscillator, *International Conference on Noise and Vibration Engineering 2012, ISMA 2012*, Leuven, Belgium, **45(2)** 563-578
[16] Yang J, Xiong Y P and Xing J T 2014 Nonlinear power flow analysis of the Duffing oscillator, *Mech. Syst. Signal Pr.* **45(2)** 563-578
[17] Yang J, Xiong Y P and Xing J T 2015 power flow behaviour and dynamic performance of a nonlinear vibration absorber coupled to a nonlinear oscillator, *Nonlinear Dynam.* **80(3)** 1063-1079
[18] Yang J 2013 Power flow analysis of nonlinear dynamical systems (PhD thesis) (Southampton: University of Southampton)